

Modeling of Fluorescent Color Mixing by Regression Analysis

Petri Turunen, Jussi Kinnunen*, Jarkko Mutanen* ; *Department of Physics and Mathematics, University of Eastern Finland, Joensuu Campus, Finland

Abstract

Modeling of fluorescent color mixing is studied by applying regression analysis to the measured bispectral data. A sample set was prepared by using three fluorescent paints and different mixing combinations. The accuracy of estimations was evaluated by calculating the color difference ΔE in the CIELAB color space and Euclidean distance of spectra. Even though the estimation errors were considerably high, the best results overall was obtained using a sparse training set and of third order terms in regression.

Introduction

Mixing of colors is common in dyeing and printing processes in textile and paper industry. In industrial processes, color management plays important role in defining product quality. In the color mixing process, the relationship between the coloration process and the resulting color should be modeled. Color mixing is divided into two different methods, subtractive and additive color mixing [1]. The additive color mixing is related to mixing of the colored lights, and subtractive color mixing to the mixing of colored pigments or dyes. For non-fluorescent dyes and pigments there are methods developed to predict the resulting subtractive color. For example a basic Kubelka-Munk [2] theory has been widely used in paper industry despite its known limitations [3–5], such as the negligence of fluorescence.

Fluorescence is a phenomenon where material is excited by electromagnetic radiation in the specific wavelength region and the excited state relaxation emits electromagnetic radiation in another, usually longer, wavelength region [6]. When the excitation wavelengths of the material are in ultraviolet (< 380 nm) region the emission wavelengths are usually in visible region (380–780 nm). The fluorescence can be measured by many methods [7] but the most accurate one, in the sense of color, is the two-monochromator method [8] which was originally developed by Donaldson in the year 1954 [9]. The result of fluorescence measurement is a Donaldson matrix which is a complete illuminant independent matrix representation of the bispectral radiance factor of the sample in the used measurement geometry where the radiance factor is expressed at each excitation and emission wavelengths. The reflectance information about the sample is located in the diagonal of the Donaldson matrix. The standardization of methods for fluorescence measurements and data analysis as the calculation of the total radiance factor has been developed [10].

Mixing of fluorescent colorants is a complex process. Because of the fluorescence, the total radiance factor of the single colorant and thus the mixed color is illuminant dependent. In addition to the absorption of pigments and scattering inside, there is fluorescence excitation in each pigment. In mixed fluorescent color the emitted light by one single colorant can cause fluorescence in another colorant. In addition, if the pigments are close enough (< 10 nm) the transition of energy can occur by dipole-dipole resonance interaction known as Förster resonance energy transfer (FRET) [11]. Mixing of fluorescent dyes and

pigments have been studied earlier by applying Kubelka-Munk theory with fluorescence extension. Ramos and Lagorio developed method based on Kubelka-Munk theory for studying fluorescence of plant leaves [12, 13]. The same correction model has been used by Verri et al. to study the fluorescence spectra from the replicas of wall paintings [14]. Shakespeare has also presented a similar type method for studying coloration in papers [15]. However, none of these studies present quantitative colorimetric error analysis.

In present study, the modeling of the fluorescent color mixing is applied, i.e. estimates for the mixed color were derived by regression analysis from the measured data of a fluorescent sample set. A sample set was prepared from fluorescent paints with different concentration ratios. The Donaldson matrix of the fluorescence was measured using a custom made bispectrometer. The color difference ΔE in CIELAB colorspace and Euclidean distance of spectra were calculated for spectral comparison under simulated D65 and A illuminations. The training sets were created using 4 different size training data and 3 different amounts of terms as variables in regression analysis.

Materials and methods

Samples

The samples were prepared by mixing three fluorescent poster paints manufactured by Asahipen Corporation. The colors of the paints were vermilion (Chinese Red), green and lemon. For better fluidity, the paints were diluted with distilled water using the water/paint dilution ratio of 3/7. The better fluidity was needed, because small 1 ml syringes were used for dosing the paints to test tubes for mixing and then to 50 mm bell class sample base. Total amount of the paint in each sample was 0.5 ml. The paint was allowed to dry freely on the bell glass. The fully dry circular sample area had a diameter ranging from 2.10 cm to 2.30 cm. During the drying process there were cracks emerging on the surface of the paint layer. The effect of the cracks in fluorescence measurement was evaluated to be negligible because of the large diameter (1.50 cm) of detecting area and the measuring geometry $0/45^\circ$. The cracks did not cast shadows because of the illumination geometry used and the portion of the cracks was small compared to the whole detecting area. Four typical samples are presented in Fig. 1.

The sample set ($n=55$) consists of three primary color samples, 27 two color mixes and 25 three color mixes. The notation $[G, Y, R]$ of the sample is used to describe the mixing ratios. In this notation G is the relative concentration of the green paint in percentages, and Y and R are the corresponding values for yellow and red paints. The mixing ratio chart was constructed so that there was nine mixes $[a, b]$, $a = \{90, 80, \dots, 10\}$, $b = \{10, 20, \dots, 90\}$ for each two color combinations and 25 mixes for all three color combinations. Three color mixes were prepared as combinations $[a, b, c]$, $[b, a, c]$ and $[b, c, a]$ where $a = \{90, 80, 70, 60, 50, 40, 20, 10\}$, $b = c = \{5, 10, 15, 20, 25, 30, 40, 45\}$ and a single $[33.3, 33.3, 33.3]$ sample. The color mixtures can be plotted in three dimensional space

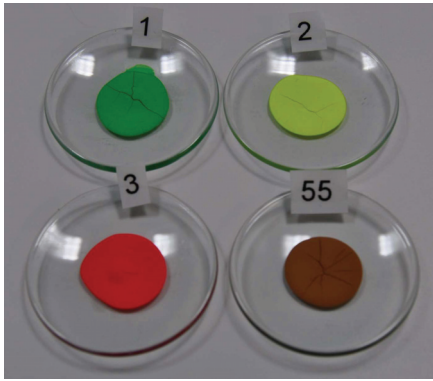


Figure 1. Four typical samples. All the three primary colors green (**top left**), lemon (**top right**), vermillion (**bottom left**) and a mixture consisting equal amount of each paint (**bottom right**).

in Fig. 2 where red dots represent all the primary colors, blue dots represent each two color mixes and green dots each three color mixes.

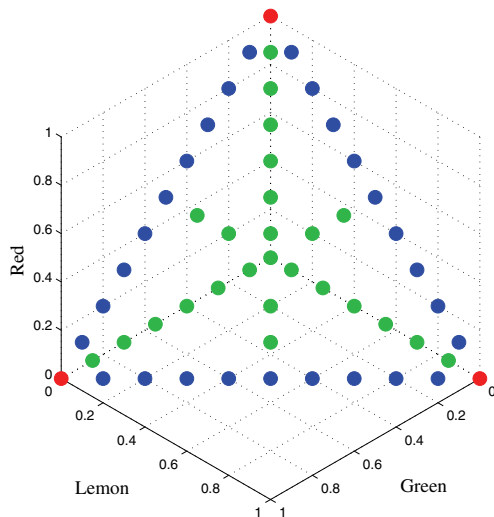


Figure 2. The constructed mixing ratio space. Red dots indicate all the primary colors, blue dots show each two color mixes, green every three color mixes.

Equipment

Fluorescence measurements were conducted by using custom made bispectrometer- a two-monochromator spectral measuring device. The bispectrometer is assembled on the optical table and currently the setup consists of 250 W Quartz Halogen lamp, Bentham DTMc300 double monochromator, Glan-Taylor polarizer, travelling table capable of holding up to four samples and Hamamatsu PMA-12 spectrograph detector with 200 – 950 nm spectral wavelength range (Fig. 3). The measuring geometry of the bispectrometer is the standard 0/45° geometry [16] and it is adjustable. The device is capable of measuring three samples and a reference simultaneously by using multiple linear polarization angles. The measurement of all samples from 300 – 800 nm with 2 nm sampling interval and two polarization angles takes approximately two hours. A custom programmed computer software is controlling the components of the bispectrometer and the data acquisition.

The excitation wavelengths used in measurements were

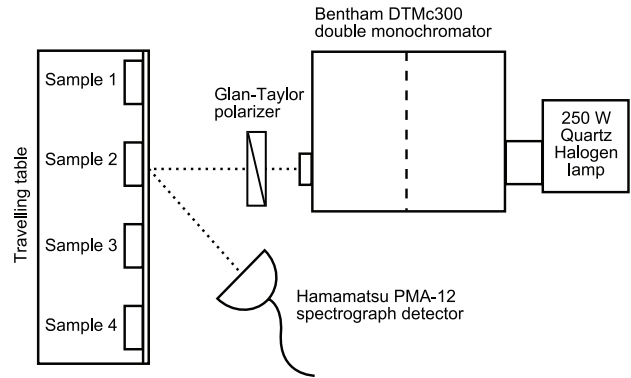


Figure 3. A principle of operation and layout of the bispectrometer.

300 – 800 nm with 2 nm sampling interval and 5 nm peak half-width. Because the fluorescence is dependent on the polarization of incident light, two linear polarization angles 0° and 90° were used. Emission spectrum for each excitation wavelength is detected in the wavelength region 200 – 950 nm. Measurements for one sample were conducted in two parts using two different exposure times. The exposure time of 80 ms was used in excitation region 300 – 400 nm, and 25 ms in the wavelength region 400 – 800 nm. To provide sufficient amount of light to the detector the 5 nm peak half-width was used. The different exposure times were necessary to compensate the spectral power distribution of the current light source (radiance decreases rapidly below 350 nm) which causes noise in the emission spectra.

Donaldson matrix analysis

The data of the fluorescence measurement for one sample is a fluorescence matrix $F(\mu, \lambda)$ where each row represents the emission spectrum at corresponding excitation wavelengths. Notations μ and λ refers to excitation and emission wavelengths respectively. The Donaldson matrix is calculated by dividing each row of the measured fluorescence matrix by the corresponding spectral intensity of light source $E_{ill}(\lambda)$ and peak half-width $E_{ill,half}(\lambda)$ as follows [10]

$$D(\mu, i) = \frac{F(\mu, i)}{E_{ill}(\lambda) E_{ill,half}(\lambda)}, \forall i = \lambda. \quad (1)$$

The final result Donaldson matrix is calculated as an average of both linear polarization angles. An example results of the bispectrometric fluorescence measurements is shown as a radiance factor graph in Fig 4. The reflected radiance factor (reflectance) is shown in the graph with a red curve on the right and its wavelength scale at the bottom of the image. The contour in the graph shows the fluorescence radiance factor. The corresponding excitation and emission wavelengths are shown on the left and at the bottom of the figure respectively. The colorbar beside the graph represents the bispectral luminescent radiance factor.

The total radiance factor of the fluorescent sample can be simulated under any light source if the spectral power distribution of the light source is known. The D65 standard daylight illumination spectra defined by Commission Internationale d'Eclairage (CIE) and CIE1931 standard observer was used in simulations. In the simulation, the reflectance is unchanged and is obtained from the diagonal of Donaldson matrix as follows

$$\beta_R(\lambda) = D(\mu = \lambda, \lambda). \quad (2)$$

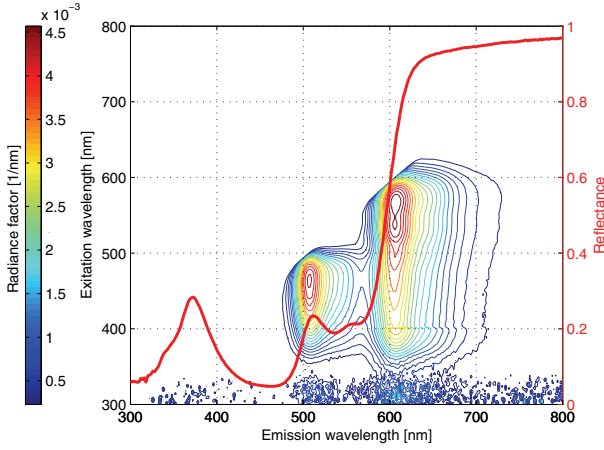


Figure 4. Radiance factor graph with the mixture of lemon and vermillion by the ratio $[0, 90, 10]$ of a sample. The excitation wavelength noise below 350 nm is caused by the low radiance of the used halogen light source.

The simulation has influence on the fluorescence part of the Donaldson matrix which is weighted by multiplying each emission spectrum with the corresponding spectral intensity of light source. The simulated fluorescence spectrum of the sample under chosen illumination is then obtained by summing up each emission spectrum of the weighted Donaldson matrix. The illuminant dependent radiance factor of fluorescence $\beta_L(\lambda)$ is calculated by dividing the summed fluorescence spectrum by the spectral intensity of the light source. The illuminant dependent total radiance factor of sample is then obtained as a sum

$$\beta_T(\lambda) = \beta_R(\lambda) + \beta_L(\lambda), \quad (3)$$

from which the XYZ-tristimulus values and further the CIELAB (L^*, a^*, b^*) color coordinates can be calculated. An example result of the simulation under D65 illumination is shown in the Fig. 5.

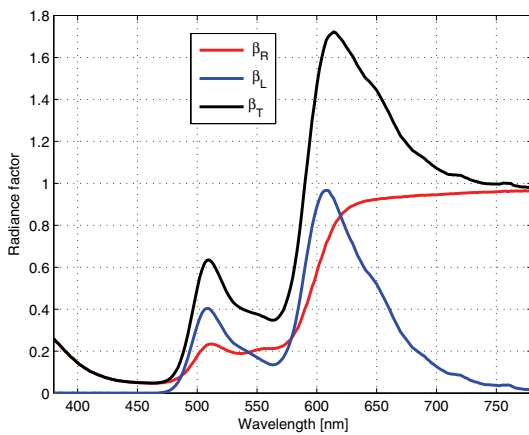


Figure 5. Simulated reflected $\beta_R(\lambda)$, luminescent $\beta_L(\lambda)$ and a total $\beta_T(\lambda)$ radiance factor spectra of sample with the mixture of lemon and vermillion by the ratio $[0, 90, 10]$ under D65 illumination.

Regression analysis

Regression analysis is a statistical method for the searching of relationships between variables [18]. The basic idea is to

create a training database by using a specific part of the known data as a training set. The testing data for the database should not be used for the creation of the database. In this study, the regression problem is solving the spectrum $\mathbf{r}_i(\lambda)$ for mixing ratio $\mathbf{s}_i = [G_i, Y_i, R_i]$ for any given ratio. A matrix \mathbf{R} size of $l \times n$ is defined from the spectra of chosen training sample set as follows

$$\mathbf{R} = \begin{bmatrix} \mathbf{r}_1(\lambda) \\ \vdots \\ \mathbf{r}_l(\lambda) \end{bmatrix}, \quad (4)$$

where each row represents a spectrum of each sample of the training sample set size of l samples. Index n represents the dimension of spectra. A matrix \mathbf{S} size of $l \times k$ from the corresponding mixing ratios is defined as

$$\mathbf{S} = \begin{bmatrix} \mathbf{s}_1 \\ \vdots \\ \mathbf{s}_l \end{bmatrix}, \quad (5)$$

where \mathbf{s}_i is a row vector and index k denotes the number of terms in the mixing ratio vector. The linear model using only the first order terms of \mathbf{s} is defined as

$$\mathbf{s}_i = [1, G_i, Y_i, R_i], k = 4, \quad (6)$$

where constant 1 is used for biasing [18]. In addition to the linear components, the 2nd or third order polynomials can be used to improve the matching of the training set. However, using a higher degree of polynomials may cause instability in the estimation model when testing the data outside the training set. When using the 2nd degree regression with all the cross-product terms the mixing ratio vector are $[1, G, Y, R, G^2, Y^2, R^2, G*Y, G*R, Y*R]$, $k = 10$. Third order polynomials are $[1, G, Y, R, G^2, Y^2, R^2, G*Y, G*R, Y*R, G^3, Y^3, R^3, G*Y^2, G^2*Y, G*R^2, G^2*R, Y*R^2, Y^2*R, G*Y*R]$, $k = 20$. The basic regression estimation model can be written as

$$\mathbf{R} \approx \mathbf{S}\mathbf{W}, \quad (7)$$

where \mathbf{W} is a transformation matrix size of $k \times n$. By using the least square fitting [18] the solution for matrix \mathbf{W} can be calculated using pseudoinverse. In this study the pseudoinverse was calculated using matlab function *pinv*. An estimate spectrum $\mathbf{r}_{test}(\lambda)$ for specific testing mixing combination \mathbf{s}_{test} is then obtained as follows

$$\mathbf{r}_{test}(\lambda) \approx \mathbf{W}\mathbf{s}_{test}. \quad (8)$$

The regression process was conducted using two calculation procedures. In the first one, called "regression from matrices" and abbreviated as "Mat", the reflectance and fluorescence parts of the Donaldson matrices were treated separately. The reflectance part of the Donaldson matrices of chosen training set samples is analyzed by simply using the reflectance spectrum as a data for each sample. The fluorescence part was analyzed so that the emission spectrum at each excitation wavelength is used as a data vector independently for one sample. Thus, the regression analysis is applied to each excitation wavelength resulting

in this case the total of 251 (300 to 800 nm with 2 nm interval) transformation matrices \mathbf{W} . The estimation of emission spectrum for the test sample is calculated individually for each excitation wavelength using Eq. 8. The estimation for fluorescence part of the Donaldson matrix is then formed from the estimated emission spectra. The simulation under different light sources is applied as described above using estimated reflectance and fluorescence parts. Total radiance factor of the estimation is obtained from Eq. 3.

In the second calculation procedure, called "regression from simulations" and abbreviated as "Sim", the measured Donaldson matrices are first simulated under different light sources. The simulated total radiance factor spectrum obtained from Eq. 3 is used as the data vector for each sample. Estimation of the simulated total radiance factor spectrum is calculated using Eq. 8. The idea behind the "Sim" method is to simulate the calculation when the total radiance factor have been obtained using polychromatic light and spectroradiometer.

Test and training sets

The test set was fixed and it is illustrated as black dots in Fig 6. The test samples were chosen intentionally in the middle area of the mixing space, where the mixing ratios of each paint are fairly equal. Four training sample sets were constructed from the rest of the samples by changing the "sparseness" of samples in the mixing ratio space around the test samples starting only with the primary colors and the middle point sample which composes equal amount of each paint. Thus, the first training set, represented as red dots in Fig 6 (a), consists of four samples which is 7.2% of total samples. In the 2nd training set, the size is increased to 16 samples (29.1% of total) by adding the three samples from each two color mixes and one sample from each three color mixes as shown as red and magenta dots in Fig 6 (b). In the third training set, the every second from each two color mixes and three samples from each three color mixes is added as shown as red, magenta and blue dots in Fig 6 (c) and the size is increased to 28 (51.1% of total). The fourth training set size of 46 samples (83.6% of total) consists of every sample except the test sample as shown as red, magenta, blue and cyan dots in Fig 6 (d).

Comparison methods

Two comparison methods, CIELAB color difference and Euclidean distance between the estimate and measured spectrum, were used to evaluate the accuracy of estimation. CIELAB color difference is a widely used measure in color inspection because of the uniformity of CIELAB color space. It is defined as an Euclidean distance between two color coordinates (L_1^*, a_1^*, b_1^*) and (L_2^*, a_2^*, b_2^*) in CIELAB color space, as follows [17]

$$\Delta E = \sqrt{(\Delta L^*)^2 + (\Delta a^*)^2 + (\Delta b^*)^2}, \quad (9)$$

where

$$\begin{aligned} \Delta L^* &= L_1^* - L_2^* \\ \Delta a^* &= a_1^* - a_2^* \\ \Delta b^* &= b_1^* - b_2^*. \end{aligned}$$

A practical interpretation of ΔE can be described in many ways, however, the evaluation of quality and acceptability requirements depends highly on application [19]. In this study, the CIELAB color coordinates were calculated by using the total radiance factors simulated under D65 and A illuminations. However, it should be noted that the CIELAB color space is designed

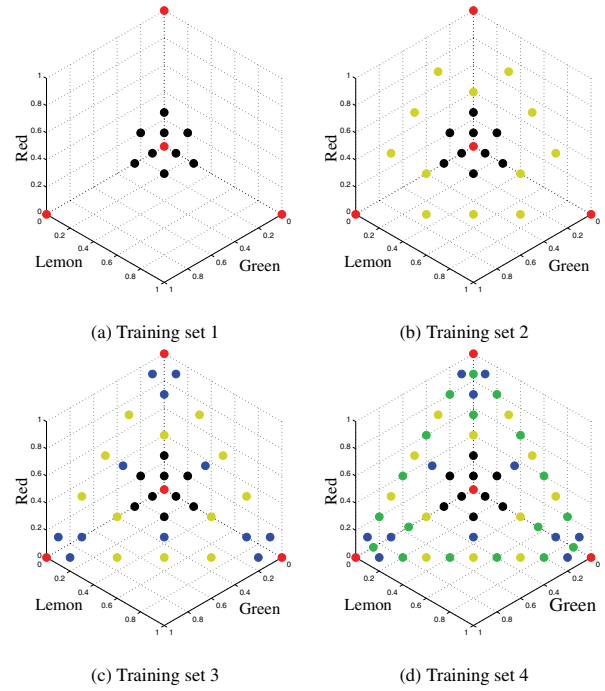


Figure 6. The constructed mixing ratio space showing samples of each training sample set and the test samples. Red dots represent the first training set (a), magenta dots show the added samples in the 2nd training set (b), blue ones show the added samples in the third training set (c) and cyan ones show the added samples in fourth training set (d).

for non-fluorescent colors. In case of fluorescent colors the value of L^* coordinate, which represents the lightness of the color can go beyond 100 which corresponds to the normalized maximum value for L^* coordinate CIELAB color space.

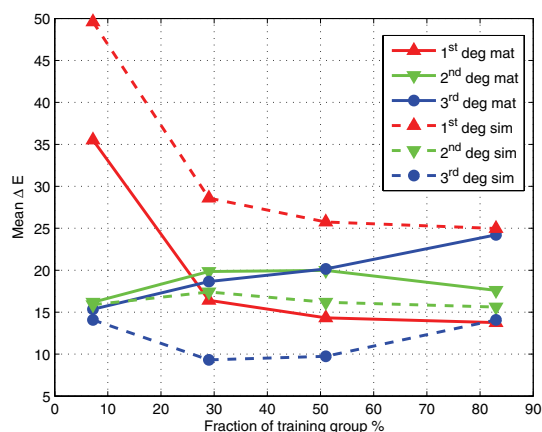
The second comparison method was Euclidean distance between spectra. The Euclidean distance is the most explicit measure for error estimation between two vectors though it has no defined meaning in a sense of color matching as the CIELAB color difference. The Euclidean distance between two spectra $\mathbf{r}_1(\lambda)$ and $\mathbf{r}_2(\lambda)$ is defined as follows

$$d(\mathbf{r}_1, \mathbf{r}_2) = \sqrt{\sum_{i=1}^n [\mathbf{r}_1(\lambda_i) - \mathbf{r}_2(\lambda_i)]^2}, \quad (10)$$

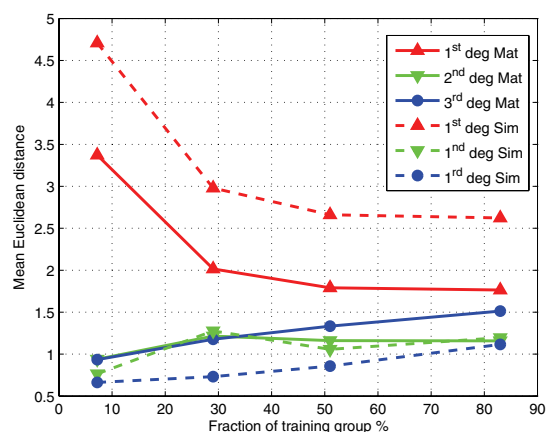
where n represents the dimension of spectra.

Experimental

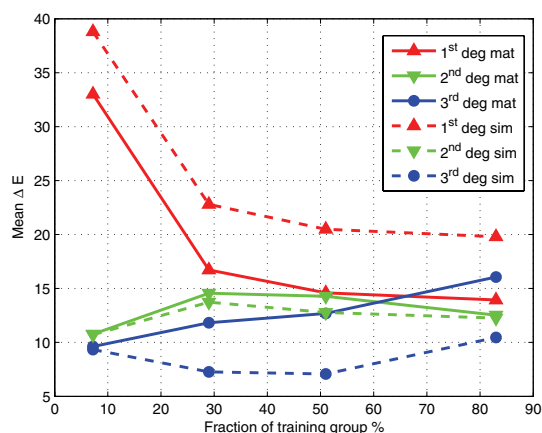
The regression analysis and the total radiance factor estimations for test samples under D65 and A illuminations were computed using both "Mat" and "Sim" methods, four training sets and one to three regression degrees as variables. The color difference ΔE and the Euclidean distance between spectra $d(\mathbf{r}_1, \mathbf{r}_2)$ were calculated for the estimated and measured total radiance factor for each test sample. The mean ΔE and the Euclidean distance for each calculation combination as a function of training set size is shown in Figs. 7 and 8 where one can notice that the linear regression is not giving as good estimations even with larger training sets than the 3rd degree regression with sparse training sets. The examples of one of the good (a) and bad (b) estimations for one sample are shown in total radiance factor graphs in Fig. 9. An example of standard deviations of ΔE under D65 illumination is shown in Fig. 10 which illustrates the high deviation of ΔE values.



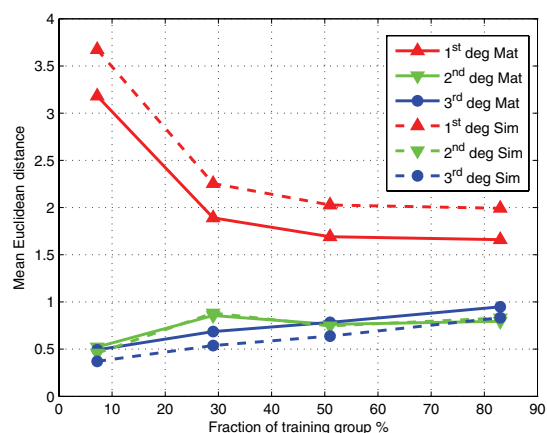
(a) D65



(a) D65



(b) A



(b) A

Figure 7. The mean ΔE between estimated and measured total radiance factor as a function of training set size with two testing methods: "Mat" where the regression is calculated before simulation by using the Donaldson matrix and "Sim" where the regression is calculated by using the radiance factor of the samples under standard illumination. D65 and A illuminants were used for simulations. The "Mat" method gives better estimate with linear degree regression and the "Sim" method with the 2nd and 3rd degree regression.

Figure 8. The mean Euclidean distance $d(r_1, r_2)$ between estimated and measured total radiance factor as a function of training set size with two testing methods: "Mat" where the regression is calculated before simulation by using the Donaldson matrix and "Sim" where the regression is calculated by using the radiance factor of the samples under standard illumination. D65 and A illuminants were used for simulations. The "Mat" method gives better estimate with linear degree regression and "Sim" method with the 2nd and 3rd degree regression.

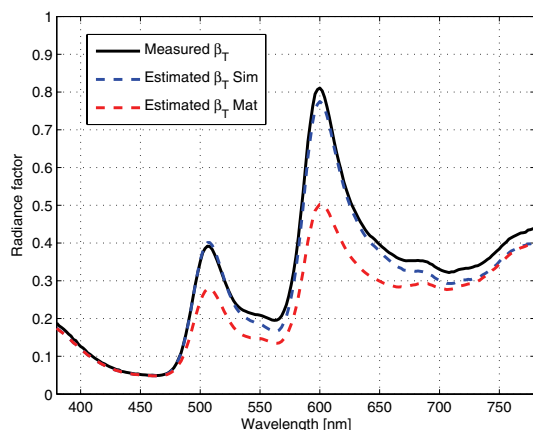
Discussion

The mean Euclidean distance in Fig. 8 have similar type shapes when comparing to ΔE mean values, differences in behavior occur mainly in the 2nd and 3rd degree regressions. The linear regression behaves the most logically as the estimation errors decrease when the training set size increase for both regression methods. The "Mat" method gives the better estimate with linear degree regression and the "Sim" method with 2nd and 3rd degree regression. The effect of overtraining is affecting especially the performance of 3rd degree regression where the error measures increases as the training set size increases. The only exceptions are the 2nd and 3rd training set for the "Sim" method which gives fairly good estimations ($\Delta E = 0.49$ being the smallest) for some samples. In overall the estimation errors are smaller under A illumination because of weak spectral intensity in the wavelength region 400 – 500 nm where the fluorescence excitation of the samples mainly occurs and thus the possible error caused by the fluorescence estimation is reduced. The deviation of ΔE in each calculation procedure is very large ranging from 4 to 12.5 as seen in Fig. 10. The estimation of some samples

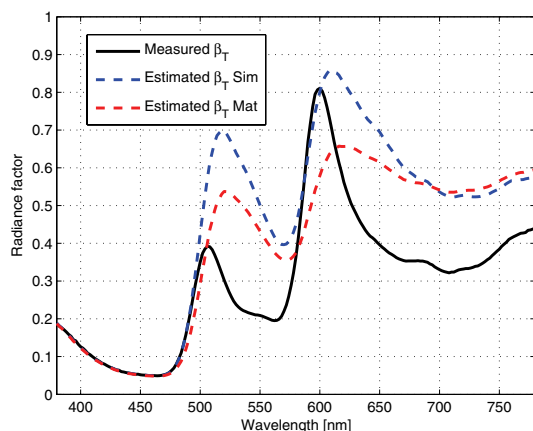
is remarkably large (> 20) in almost every calculation procedure. That indicates that the irregularity of the measured data is high. The sample preparation was made completely manually and errors can arise from the preparation. In addition, the drying process of the samples affected the surface flatness which causes differences in the measurements because of the local measurement geometry variations.

In the example of good estimation in Fig. 9 (a), the total radiance factor estimated using the "Sim" method follows the measured one accurately. The effects of bad estimation in spectra are clearly visible from the bad estimation example in Fig. 9 (b). The peak intensities and positions of both estimate spectrum differ considerably from the measured spectrum.

By using the regression analysis the mean ΔE values are high (Fig. 7) and not satisfactory, in the means of color matching, even at the lowest points. However, a comparison to other methods such as the fluorescence-extended Kubelka-Munk method is impossible because the lack of quantitative analysis of color differences in studies [12–15] where the fluorescence-extended



(a) Good estimation, $\Delta E = 2.58$ ("Sim") and $\Delta E = 16.93$ ("Mat")



(b) Bad estimation, $\Delta E = 33.71$ ("Sim") and $\Delta E = 22.82$ ("Mat")

Figure 9. The estimated and measured total radiance factors of test sample [25,50,25]. The example of good estimation ($\Delta E = 2.58$ with "Sim" method, $\Delta E = 16.93$ with "Mat" method) under D65 presented in the graph (a). The estimations are calculated using the 2nd training set and the 3rd regression degree. The example of bad estimation ($\Delta E = 33.71$ with "Sim" method, $\Delta E = 22.82$ with "Mat" method) presented in the graph (b). The estimations are calculated using the first training set and the linear regression.

Kubelka-Munk model was applied. To our knowledge, there is no earlier study that models the reproduction of fluorescent color mixtures by colorimetric analysis.

Conclusions

The purpose of this work was to study how the regression analysis can be applied to model the fluorescent color mixing accurately. It has been shown that as the linear regression behaves the most logically, thus, the higher degree regressions perform better when using sparser training sets. The standard deviation of error between samples is high (from 4 to 12.5 for ΔE). The reason for big variances and estimation errors can be the irregularity of samples, caused by inaccuracy in the dosing of paint process and the limited number of fixed samples which is an issue because of the regression method.

In mathematical and statistical sense, the most accurate method to analyze the data set by using the regression analysis is to choose the training samples randomly multiple times using the specific training set sizes and use the rest of the data as a test data. However, considering the physical point of view, it is more

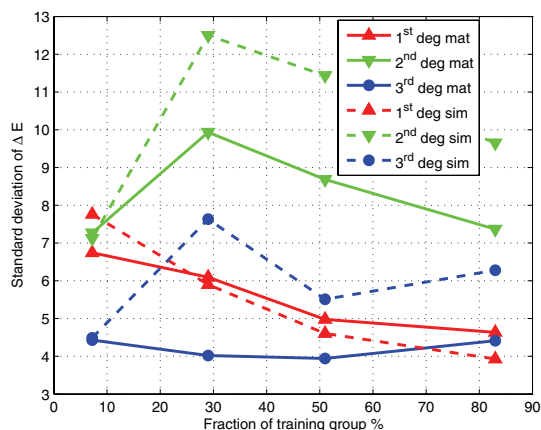


Figure 10. The standard deviation of ΔE between estimated and measured total radiance factor as a function of training set size with two testing methods: "Mat" where the regression is calculated before simulation by using the Donaldson matrix and "Sim" where regression is calculated by using the radiance factor of the samples under D65 standard illumination.

informative to study how the training set consisting of primary colors or some simple mixes can predict the more complex color mixing combinations accurately. That is the reason why the fixed test sample group in this study was used. Based on the present study, if the regression is used, a sparse training set and 3rd order terms using already simulated total radiance factors would give the best result for the spectrum prediction of three pigment mixture.

References

- [1] R. S. Berns, Billmeyer and Saltzman's principles of color technology, John Wiley and Sons, New York, 2000.
- [2] P. Kubelka and F. Munk, Ein Beitrag zur Optik der Farbanstriche, Zeits. F. Tech. Physik, 12, 593 (1931).
- [3] J. L. Saunderson, Calculation of the Color of Pigmented Plastics, J. Opt. Soc. Am. , 32, 727–729 (1942).
- [4] P. Kubelka, New Contributions to the Optics of Intensely Light-Scattering Materials. Part I, J. Opt. Soc. Am. , 38, 448 (1948).
- [5] P. Kubelka, New Contributions to the Optics of Intensely Light-Scattering Materials. Part II: Nonhomogeneous Layers, J. Opt. Soc. Am. , 48, 330–334 (1998).
- [6] G. Blasse and B. Grabmeier, Luminescent Materials, Springer-Verlag, Berlin, 1994.
- [7] J. Mutanen, Fluorescent Colors, Ph.D Thesis, University of Joensuu, Joensuu, 2004.
- [8] J. E. Leland and N. L. Johnson and A. V. Arcchi, Principles of bispectral fluorescence colorimetry, SPIE, (1997).
- [9] R. Donaldson, Spectrophotometry of fluorescent pigments, British Journal of Applied Physics, 5, 210–215 (1954).
- [10] CIE 182:2007, Calibration methods and photoluminescent standards for total radiance factor measurements, Commission Internationale de L'Eclairage, (2007).
- [11] A. P. Demchenko, Introduction to fluorescence sensing, Springer, 2008.
- [12] M. G. Lagorio, L. E. Dixelio, M. I. Litter and E. S. Roman, Modeling of Fluorescence quantum yields of supported dyes. Aluminium carboxyphthalocyanine on cellulose, J. Chem. Soc., Faraday Trans, 94, 419–425(1998).
- [13] M. E. Ramos and M. G. Lagorio, True fluorescence spectra of leaves, Photochem. Photobiol. Sci., 3, 1063–1066 (2004).
- [14] G. Verri, C. Clementi, D. Comelli, S. Cather and F. Pique, Correc-

- tion of Ultraviolet-Induced Fluorescence Spectra for the Examination of Polychromy, *Applied Spectroscopy*, 62, 1295–1302 (2008).
- [15] T. Shakespeare and J. Shakespeare, A Fluorescent extension to the Kubelka-Munk Model, *Color Res. Appl.*, 28, 4–14 (2002).
- [16] R. Hunt, *Measuring Colour*, Fountain Press, England, 1998.
- [17] P. G. Cielo, *Optical techniques for industrial inspection*, SPIE, USA, 1986.
- [18] T. Hastie, R. Tibshirani, J. Friedman, *The Elements of Statistical Learning: Data Mining, Inference, and Prediction*, Springer, New York, 2001, pg. 214.

- [19] J. Y. Hardeberg, *Acquisition and Reproduction of Color Images: Colorimetric and Multispectral Approaches*, Dissertation.com, USA, 2001.

Author Biography

Petri Turunen received his MSc in physics from University of Eastern Finland in spring 2010. The subject of his MSc thesis was related to the modeling of fluorescent color mixing. He worked as a research assistant in a color research group at the University of Eastern Finland from summer 2009 to spring 2010.